A Revised Method of Presenting Wavenumber-Frequency Power Spectrum Diagrams That Reveals the Asymmetric Nature of Tropical Large-scale Waves

Winston C. Chao

Laboratory for Atmospheres, NASA/Goddard Space Flight Center

Greenbelt, MD 20771

Bo Yang and Xiouhua Fu

International Pacific Research Center

School of Ocean and Earth Science and Technology

University of Hawaii at Manoa

Honolulu, HI 96822

(Submitted to Climate Dynamics, May 14, 2008)

Corresponding Author Address:
Dr. Winston C. Chao
Mail Code 610.1
NASA/Goddard Space Flight Center
Greenbelt, MD 20771
Winston.c.chao@nasa.gov

Abstract

The popular method of presenting wavenumber-frequency power spectrum diagrams for studying tropical large-scale waves in the literature is shown to give an incomplete presentation of these waves. The so-called "convectively-coupled Kelvin (mixed Rossby-gravity) waves" are presented as existing only in the symmetric (anti-symmetric) component of the diagrams. This is obviously not consistent with the published composite/regression studies of "convectively-coupled Kelvin waves," which illustrate the asymmetric nature of these waves. The cause of this inconsistency is revealed in this note and a revised method of presenting the power spectrum diagrams is proposed. When this revised method is used, "convectively-coupled Kelvin waves" *do* show anti-symmetric components, and "convectively-coupled mixed Rossby-gravity waves (also known as Yanai waves)" *do* show a hint of symmetric components. These results bolster a published proposal that these waves should be called "chimeric Kelvin waves," "chimeric mixed Rossby-gravity waves," etc. This revised method of presenting power spectrum diagrams offers an additional means of comparing the GCM output with observations by calling attention to the capability of GCMs to correctly simulate the asymmetric characteristics of equatorial waves.

1 Introduction

Tropical large-scale waves, both observed and modeled, have been analyzed by the power-spectrum analysis method and presented in the form of wavenumber-frequency power-spectrum diagrams (e.g., Hayashi 1982, Takayabu 1994). To make the tropical waves stand out in these diagrams, Wheeler and Kiladis (1999; hereafter WK) constructed a background power spectrum (their Fig. 2) by averaging the "raw" power spectra of the symmetric (with respect to the equator) and anti-symmetric components (their Fig. 1) and then applying, many times, a 1-2-1 smoothing filter in both frequency and wavenumber domains. For each of the symmetric and anti-symmetric components, the ratio of the "raw" power spectrum to the same background power spectrum is then presented as the final power spectrum (their Fig. 3). The WK method of presenting wavenumber-frequency power spectrum diagrams has become popular among researchers who compare GCM model output with observations (e.g., Lin et al. 2006). However, despite its popularity, this method can be improved upon.

In their Fig 3, what WK identified as "convectively-coupled Kelvin waves" are seen only in the symmetric component of their diagrams, and what WK identified as "convectively-coupled mixed Rossby-gravity waves" (also known as Yanai waves) are seen only in the anti-symmetric component of their diagrams. However, in the composite/regression analysis of "convectively-coupled Kelvin waves" by Straub and Kiladis (2002, their Fig. 16), these waves are clearly not symmetric with respect to the equator, and thus should have both symmetric and anti-symmetric components in the wavenumber-frequency power spectrum diagrams. This asymmetry is obvious from the

fact that these waves are associated with oscillations within ITCZs, and ITCZs are rarely symmetric with respect to the equator. In fact, if one examines Fig. 1 of WK, the "raw" power spectra, closely; it is discernable that in the anti-symmetric component there is a local peak at an approximate frequency of 0.22 cpd (cycles per day) and eastward wavenumbers 6 and 7 (this spot in the diagram is hereafter referred to as the F0.22E6-7 spot), corresponding to the "convectively-coupled Kelvin waves."

This note explains the reason why Fig. 3 of WK does not reveal the asymmetric nature of the convectively-coupled Kelvin and mixed Rossby-gravity waves, and offers a revised method of presenting the power spectra that does reveal the asymmetric nature of these waves. It also provides the wavenumber-frequency spectral diagrams constructed with our revised method. This note concludes with some remarks of our findings.

2 The cause of the discrepancy and a solution

The cause of the above-mentioned discrepancy lies in the way the background power spectrum is constructed. When constructing the background power spectrum, WK averaged of the "raw" power spectra of the symmetric and anti-symmetric components and applied a smoothing filter many times to the average to obtain a single background power spectrum. WK then used the same background power spectrum for both the symmetric and anti-symmetric components when they divided the "raw" power spectra of these components by the background power spectrum to obtain their final spectral diagrams (Fig. 3 of WK). The use of thus-constructed background has obscured the anti-symmetric component of "convectively-coupled Kelvin waves." For example, the local

weak peak in the "raw" anti-symmetric diagram (Fig. 1a of WK) at F0.22E6-7 was divided by a large background, which has a large contribution from the symmetric component, and therefore it is not seen as a peak at all in the resulting ratio, as presented in Fig. 3a of WK.

The solution to this discrepancy is to revise the method of constructing the background in two steps. One is to use separate background spectra for the symmetric and anti-symmetric components. For each component, the background spectrum should be constructed from filtering its own "raw" power spectrum. The other step is, instead of filtering the "raw" power spectrum of each component, to filter the 10-based logarithm of the "raw" power spectrum of each component many times and then to take the 10-based exponential of the filtered results--to get each background.

The first step is necessary because the intent of constructing the background is to use it to compare with (i.e., either to subtract from or to divide) the "raw" power spectrum to make the local peaks in the "raw" power spectrum stand out. The "raw" spectrum of the other component should play no role in constructing the background of this particular component. Hence, it is more logical to use the symmetric and anti-symmetric components separately to construct the background for each component. The second step is necessary because the "raw" power spectrum has, in most of the wavenumber-frequency domain, an exponential-like distribution in both the frequency and wavenumber directions (which is the reason the 10-based logarithm was used in WK's Figs. 1 and 2), and the 1-2-1 filter applied to the "raw" power spectrum tends to create a false increase in the magnitude of the background power spectrum. In essence, when a 1-2-1 filter is applied to an exponential function, it increases the value of the

exponential function. The new figure--which corresponds to WK's Figure 3--presents, for each of the symmetric and anti-symmetric components, the ratio of the "raw" spectrum to its new background.

3 The spectral diagrams obtained with the revised method

We revised WK's computer code, provided by M. Wheeler, according to our two-step revision. Also, we used the daily outgoing longwave radiation (OLR) dataset of Liebmann and Smith (1996) from 1979 to 1996. The data resolution was 2.5° latitude by 2.5° longitude. Data from 15°S to 15°N were used. The results, corresponding to Fig. 3 of WK (i.e., the ratios between the "raw" power spectra and the new backgrounds), are shown in Fig. 1. The corresponding power-spectrum diagrams without our revision are given in Fig. 2 for comparison purpose. Two whited-out rectangular areas on the right side of the diagrams are not plotted; the reason for this was given on page 377 of WK. Fig. 2 does not match WK's Fig. 3 exactly. This may be due to the different manner of data handling prior to the use of the WK code. However, Fig. 2 is generally consistent with WK's Fig. 3. The peak values for "convectively-coupled Kelvin waves" and "mixed Rossby-gravity waves" are lower in Fig. 1 than in Fig. 2. This is a result of the fact that in the peak regions in Fig. 2, the background is lower than those computed with our method.

As expected, Fig. 1a shows that the "convectively-coupled Kelvin waves" now also have anti-symmetric components, as indicated by the peak at the F0.22E6-7 spot. This peak has a magnitude slightly above 1.1 (i.e., the "raw" power being 10 percent

above the background), a level considered by WK as statistically-significant. Since at the peak regions of the diagrams, our backgrounds have higher values than that obtained via the WK method, a value greater than 1.1 in our diagrams is more statistically-significant than the same value using the WK method. The special dotted contour line that has a value of 1.05 surrounding the F0.22E6-7 peak indicates that this peak region is aligned with the same Kelvin wave dispersion line of 25 m equivalent depth (shown as a dashed straight line) as the symmetric "convectively-coupled Kelvin waves". This alignment becomes even more clear when only northern summer data are used, as discussed in the next paragraph. Thus, this peak region is a reflection of the anti-symmetric component of the "convectively-coupled Kelvin waves." This peak in Fig. 1a is completely missing in Fig. 2a. The "convectively-coupled mixed Rossby-gravity waves" now also have a hint of symmetric components, as indicated by the weak peak at F0.29E0, which lies close to the dispersion curve of the mixed Rossby-gravity wave of 25 m equivalent depth (the dashed curve in Fig. 1b). Also noteworthy is the fact that the anti-symmetric components of both the "convectively-coupled equatorial Rossby waves" and the MJO are stronger in Fig. 1a than in Fig. 2a. The peak at F0.26W5 in Fig. 1a--easily seen in Fig. 2a also, but shifted slightly to westward wavenumber 6 in WK's Fig. 3a--is called by WK a "tropical depression" mode. Unlike the peak at F0.22E6-7, it does not have a counterpart in the symmetric diagram, Fig. 1b. It is also noted that Fig. 1a shows the antisymmetric component of the equatorial Rossby waves, which is not obvious in Fig. 2a.

When Fig. 1 is redone with data of the Jun-Jul-Aug season only (i.e., only the 96-day segments with mid-date in the JJA season are used), the results (Fig. 3a) show that the anti-symmetric component has much stronger values in the region covering the

F0.22E6-7 spot. This shaded region with values greater than 1.1 has an orientation following the Kelvin waves normal mode line corresponding to an equivalent depth of about 25 m in Fig. 3b). Therefore, this region is a distinct counterpart to the "convectively-coupled Kelvin waves" in the symmetric diagram (Fig. 3b), which is a reflection of the existence of the anti-symmetric component of the "convectively-coupled Kelvin waves" (which is the most significant result of our study). This is consistent with the fact that ITCZs are more asymmetric in the JJA season. In the symmetric component, the minor peak at the F0.29E0 spot exists in the JJA season, with a peak value just over 1.1, but is shifted slightly toward eastward wavenumber 1 in the DJF season (Figs. 3b and 4b).

Notice that for either the anti-symmetric or the symmetric component, the backgrounds for the two seasons are not the same. One needs to keep this in mind when comparing Fig. 3 and Fig. 4. The anti-symmetric peak at F0.26W5 is easily recognized in the DJF season, but is barely discernable in the JJA season.

4 Remarks

The above outcome suggests that the term "convectively-coupled Kelvin waves" is inappropriate. This is because the term "Kelvin waves" has the connotation of being symmetric and having no meridional wind components. Chao (2007) has proposed that a better descriptor for "convectively-coupled Kelvin waves" is chimeric Kelvin waves, based on the fact that even in a symmetric "convectively-coupled Kelvin wave" there is a sizeable Rossby-wave component. The point made in this note further bolsters the use of

the term chimeric Kelvin waves and the other similar terms: chimeric Rossby waves and chimeric mixed Rossby-gravity waves. Together these waves may be called chimeric equatorial waves. The adjective chimeric means "composed of parts of different origin." The observed "convectively-coupled Kelvin waves," being asymmetric, contain not only Kelvin waves and Rossby waves, but also an anti-symmetric component that has no corresponding linear wave solutions. Thus, chimeric Kelvin waves is a better descriptor. The name Kelvin is retained to acknowledge the fact that these waves are eastward-moving. The modifier "convectively-coupled" can be omitted for the sake of brevity.

The significance of pointing out the above findings is that in the attempt to explain the origin of tropical large-scale waves, it is helpful to have a deeper insight into the observed properties of these waves. Also, our revised method of presenting the spectral diagrams of chimeric equatorial waves offers an additional means of comparing the GCM output with observations by calling attention to the capability of the GCMs to correctly simulate the asymmetric characteristics of these waves (i.e., their capability to correctly simulate the peak at F0.22E6-7 in the anti-symmetric diagram (Fig. 1a, and the corresponding region in Fig. 3a).).

Acknowledgments. Winston Chao was supported by the Modeling, Analysis and Prediction program of NASA Science Mission Directorate. Bo Yang and Xiouhua Fu were supported by the NASA Earth Science Program, NSF Climate Dynamics Program, and IPRC. IPRC is sponsored by NASA, NOAA, and the Japanese Agency for Marine-Earth Science and Technology (JAMSTEC). Matthew Wheeler provided the WK code

for the wavenumber-frequency diagram. Myong-In Lee, Phil Pegion, and Baode Chen of NASA/Goddard/GMAO provided their versions of the WK code for reference purposes. The OLR data used were from Liebmann and Smith of NOAA/CDC.

References

Chao WC (2007) Chimeric equatorial waves as a better descriptor for "convectively-coupled equatorial waves". J Meteor Soc Japan 85: 521-524

Hayashi Y (1982) Space-time spectral analysis and its applications to atmospheric waves. J Meteor Soc Japan 60: 156-171

Lin J-L, et al. (2006) Tropical intraseasonal variability in 14 IPCC AR4 climate models. Part I: Convective signals. J Climate 19: 2665-2690

Liebmann B, Smith CA (1996) Description of a complete (interpolated) outgoing longwave radiation dataset. Bull Amer Meteor Soc 77: 1275-1277

Straub KH, Kiladis GN (2002) Observations of a convectively-coupled Kelvin wave in the eastern Pacific ITCZ. J Atmos Sci 59: 30–53.

Takayabu YN (1994) Large-scale cloud disturbances associated with equatorial waves. Part I.: Spectral features of the cloud disturbances. J Meteor Soc Japan 72: 433-448

Wheeler MC, Kiladis GN (1999) Convectively-coupled equatorial waves: Analysis of clouds and temperature in the wave-number-frequency domain. J Atmos Sci 56: 374-399

Figure Captions

Fig. 1. Zonal wavenumber-frequency diagram of (a) antisymmetric and (b) symmetric OLR spectral power divided by a background constructed with the revised method. Superimposed are the dispersion curves for the first (a) even and (b) odd meridional mode for equivalent depths of 12, 25, and 50 m. The 25 m dispersion curve for the Kelvin waves is drawn in (a) as a dashed line and that for the mixed Rossby-gravity waves is drawn in (b) as a dashed curve. The dotted contour line surrounding the F0.22E6-7 region in (a) has a value of 1.05.

Fig. 2. Same as Fig. 1, but the background was constructed with the WK method.

Fig. 3. Same as Fig. 1, but only JJA data have been used.

Fig. 4. Same as Fig. 1, but only DJA data have been used.

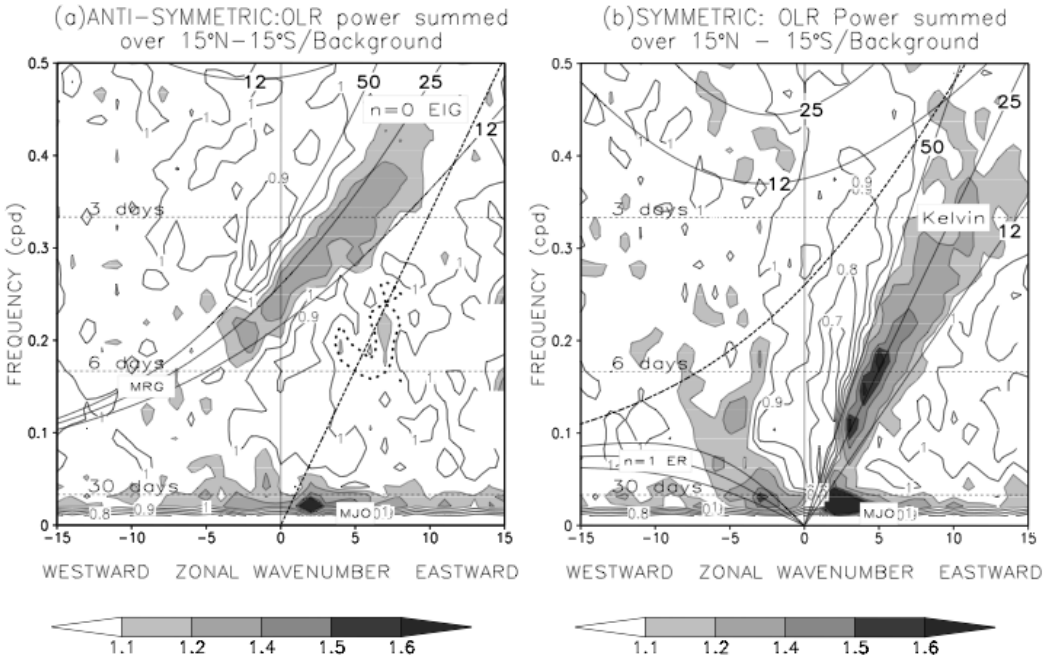

Fig. 1. Zonal wavenumber-frequency diagram of (a) antisymmetric and (b) symmetric OLR spectral power divided by a background constructed with the revised method. Superimposed are the dispersion curves for the first (a) even and (b) odd meridional mode for equivalent depths of 12, 25, and 50 m. The 25 m dispersion curve for the Kelvin waves is drawn in (a) as a dashed line and that for the mixed Rossby-gravity waves is drawn in (b) as a dashed curve. The dotted contour line surrounding the F0.22E6-7 region in (a) has a value of 1.05.

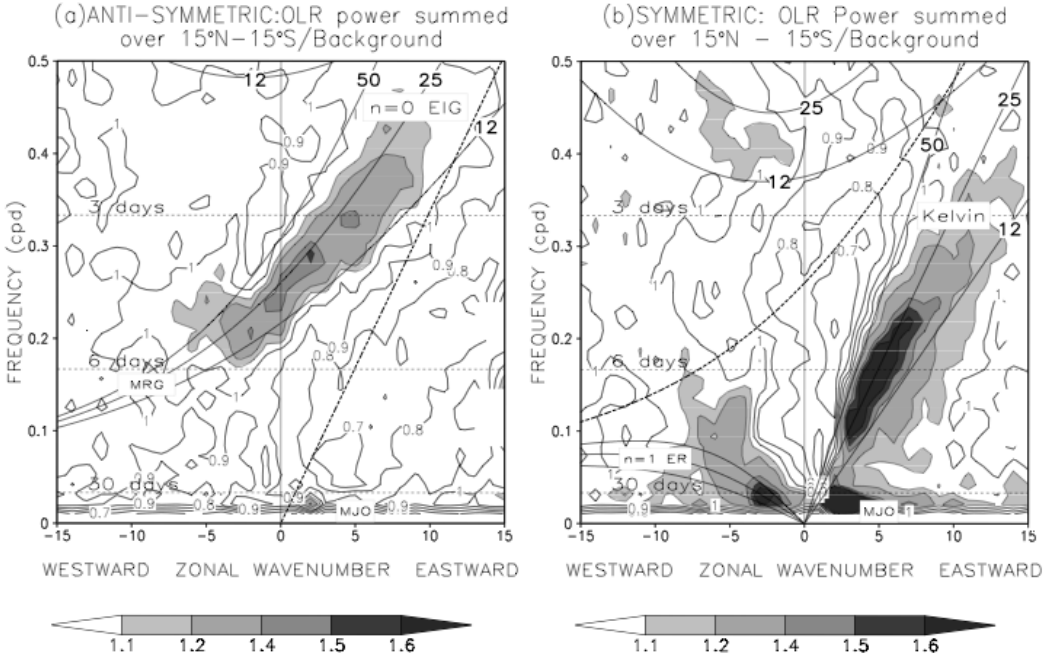

Fig. 2. Same as Fig. 1, but the background was constructed with the WK method.

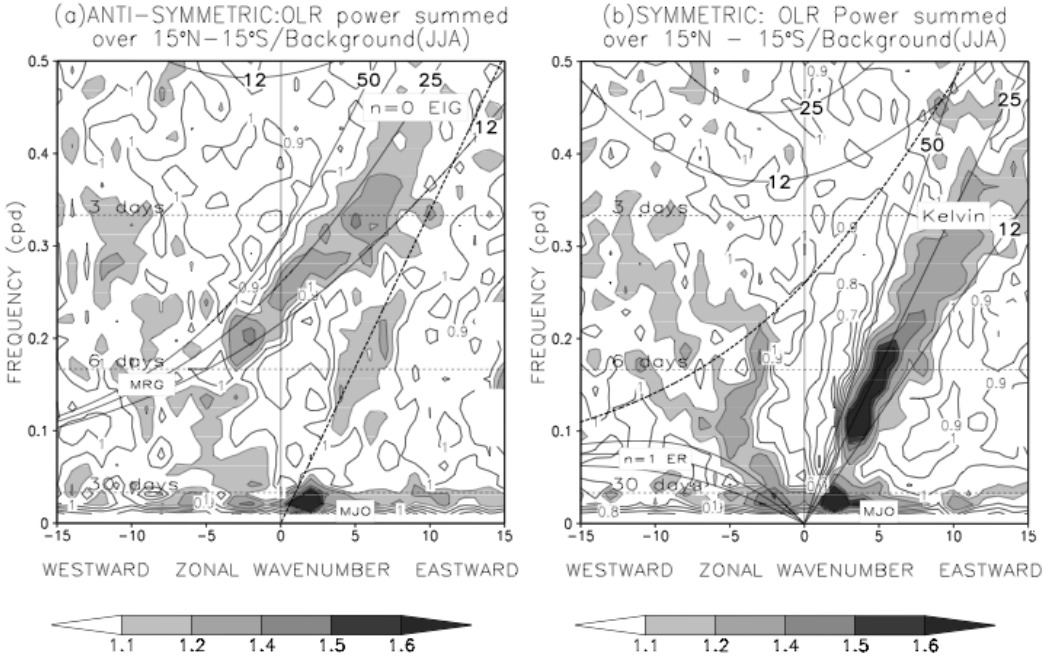

Fig. 3. Same as Fig. 1, but only JJA data have been used.

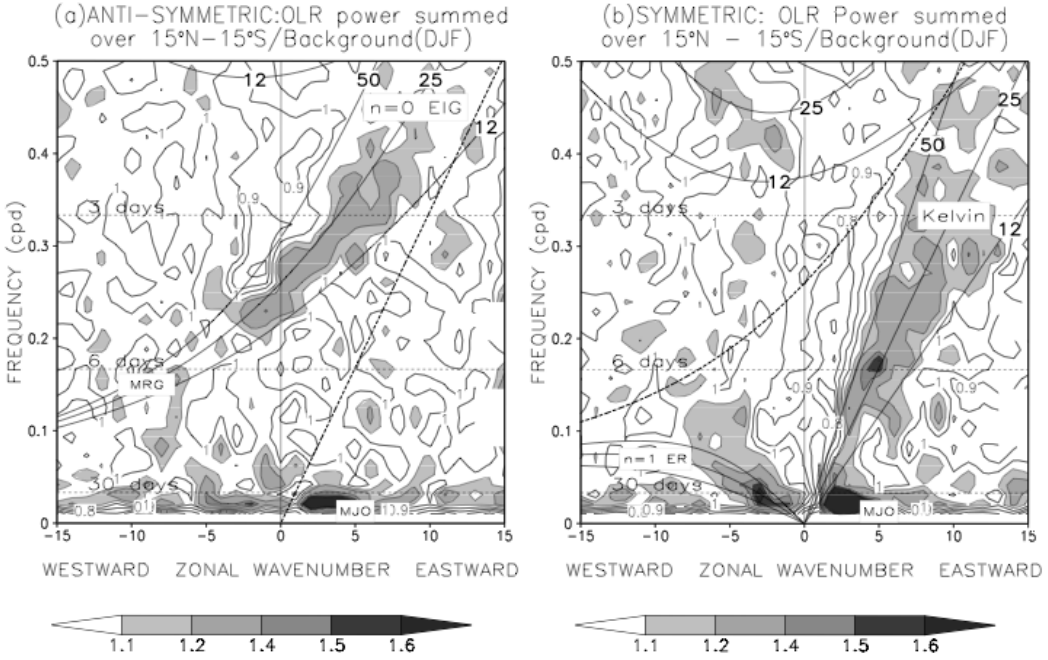

Fig. 4. Same as Fig. 1, but only DJA data have been used.